

Mesoscale fronts as foraging habitats: composite front mapping reveals oceanographic drivers of habitat use for a pelagic seabird

Kylie L. Scales^{1*}, Peter I. Miller¹, Clare B. Embling², Simon N. Ingram², Enrico Pirotta³
& Stephen C. Votier^{4*}

1. Plymouth Marine Laboratory, Prospect Place, Plymouth, PL1 3DH, UK

2. Marine Biology and Ecology Research Centre, University of Plymouth, Plymouth, PL4 8AA, UK

3. Institute of Biological and Environmental Sciences, University of Aberdeen, Aberdeen, AB24 2TZ, UK

4. Environment and Sustainability Institute, University of Exeter, Cornwall Campus, Penryn, TR10 9EZ, UK

* **Corresponding authors.** Emails: kysc@pml.ac.uk ; s.c.votier@exeter.ac.uk

Total word count : 6976

No. figs: 4 + 5 supplemental

No. tables: 2 supplemental

No. references: 73

SUMMARY

1 The oceanographic drivers of marine vertebrate habitat use are poorly understood yet
2 fundamental to our knowledge of marine ecosystem functioning. Here we use composite front
3 mapping and high-resolution GPS tracking to determine the significance of mesoscale
4 oceanographic fronts as physical drivers of foraging habitat selection in northern gannets *Morus*
5 *bassanus*. We tracked 66 breeding gannets from a Celtic Sea colony over two years and used
6 residence time (RT) to identify area-restricted search (ARS) behaviour. Composite front maps
7 identified thermal and chlorophyll-a mesoscale fronts at two different temporal scales – (a)
8 contemporaneous fronts and (b) seasonally persistent frontal zones. Using Generalised Additive
9 Models (GAM), with Generalised Estimating Equations (GEE-GAM) to account for serial
10 autocorrelation in tracking data, we found that gannets do not adjust their behaviour in response
11 to contemporaneous fronts. However, ARS was more likely to occur within spatially predictable,
12 seasonally persistent frontal zones (GAM). Our results provide proof-of-concept that composite
13 front mapping is a useful tool for studying the influence of oceanographic features on animal
14 movements. Moreover, we highlight that frontal persistence is a crucial element of the formation
15 of pelagic foraging hotspots for mobile marine vertebrates.

16

17 KEY WORDS

18 seabird, marine vertebrate, foraging, remote sensing, oceanographic front, habitat use

19 **1.0 INTRODUCTION**

20 Marine predators, such as seabirds, cetaceans, pinnipeds, turtles and sharks, must locate sparsely-
21 distributed prey in vast, heterogeneous and dynamic oceans. Although these diverse taxa differ
22 greatly in foraging ecology, shared scale-dependent foraging strategies have evolved, presumably in
23 response to the patchy, hierarchical distribution of pelagic prey (1-3). These strategies enable
24 predators to locate broad-scale foraging grounds and then adjust the scale of search effort to find
25 prey aggregations nested within (3, 4). Prey distributions are somewhat predictable at large- and
26 meso-scales (10s-100s km; 5), but less so at sub-mesoscales (~1km; 1, 6), which may explain why
27 foraging-site fidelity at large- and meso-scales is common among marine vertebrates (e.g. seabirds,
28 turtles, seals; 5,7-10).

29

30 Oceanographic processes operating over a range of spatial and temporal scales regulate pelagic prey
31 availability, and predictability, driving patterns of habitat utilisation for highly mobile marine
32 predators. For instance, a taxonomically diverse range of marine vertebrates is known to associate
33 with meso- (10s-100s kms) and sub-mesoscale (~1km) oceanographic features such as fronts and
34 eddies (5, 11-17). Fronts are transitions between water masses, which manifest at the surface as
35 horizontal gradients in temperature, salinity, density, turbidity or colour (18, 19). Nutrient retention
36 within fronts can significantly enhance primary production (18, 20) and bio-physical coupling leads
37 to aggregation and proliferation of zooplankton (21, 22). These conditions are suitable for pelagic
38 fish, which in turn are prey for higher predators, and hence, fronts may be foraging hotspots (18,
39 23). Despite the assumed significance of fronts as foraging locations, we still have a poor grasp of
40 their ecological value for higher trophic level predators. Fronts occur throughout the oceans, yet
41 differ considerably in strength, persistence, size and spatial variability (19). This variability, as well as
42 temporal and spatial lags in bio-aggregative effects (18, 21, 24), influences the suitability of fronts
43 for foraging, particularly for piscivores. Persistent fronts are assumed to present more predictable
44 foraging opportunities than small-scale, ephemeral and/or superficial features (25, 26), but direct
45 tests of the significance of frontal predictability for predator foraging are lacking.

46

47 Recent methodological developments can address this discrepancy. Bio-logging technology and
48 associated analytical techniques have enabled remote monitoring of individual animal distribution
49 and behaviour, enriching our insight into habitat use by marine predators (27). However, a key
50 constraint is the lack of data describing oceanographic processes and pelagic prey distributions at
51 matching spatio-temporal scales. Although *in-situ* studies have yielded valuable insights into the
52 fine-scale mechanisms underlying animal-oceanography interactions (e.g. 28-31), this eulerian

53 approach cannot provide information on behaviour throughout a foraging bout, limiting our
54 understanding of broader-scale oceanographic influence. Remotely-sensed data can supplement
55 bio-logging, identifying physical conditions that drive habitat selection in virtual real-time. Sea
56 surface temperature (SST) and chlorophyll-a (chl-a) imagery are most widely used (12, 32), but it is
57 questionable whether these metrics are appropriate for defining foraging habitat, particularly for
58 piscivores (33). Indeed, the use of chl-a imagery in shallow shelf seas could be misleading, as sub-
59 surface chlorophyll maxima in stratified areas can present more attractive foraging opportunities
60 than mixed waters with elevated surface chl-a (28). In contrast, sub-surface processes occurring
61 along thermal fronts are known to increase prey accessibility for diving predators. Convergent flow
62 fields and fine-scale downwelling aggregate plankton in the shallow thermocline (21, 22), attracting
63 higher trophic level consumers, including foraging seabirds (34, 35). Front mapping is able to detect
64 the surface profile of these important sub- and near-surface biophysical processes and is, therefore,
65 a potentially powerful tool for identifying pelagic foraging hotspots.

66

67 Composite front mapping (36) is a step forward in automated front detection via remote sensing,
68 addressing the limitations of precursor methods. To date, the majority of studies including a
69 measure of frontal activity have either identified fronts manually or used single-image edge
70 detection (SIED; 37) on single-day (e.g. 38) or temporally averaged (e.g. 16) images. However,
71 limitations of these methods reduce their utility. For example, using single-day imagery can result in
72 sacrifice of tracking data owing to cloud cover. Furthermore, temporally averaged imagery masks
73 spatiotemporal dynamics of fronts, which can be highly variable in shelf seas, giving only an
74 estimated average position of a wandering feature. Using SST/chl-a gradients it is not possible to
75 recognise contiguous curvilinear frontal features and, when using temporally averaged images, can
76 result in erroneous frontal locations. Composite front mapping (36) addresses these limitations,
77 enabling objective, automatic front detection over a sequence of images, removing cloud influence
78 and allowing for the visualisation of frontal dynamics. In addition, high-resolution front metrics,
79 such as the distance to the closest front or density of detected fronts, can be derived. These metrics
80 facilitate objective quantification of the strength of predator-frontal associations and exploration of
81 the effects of spatial scale, persistence, and magnitude of cross-frontal gradient, not always possible
82 previously.

83

84 Here we use composite front mapping and high-resolution GPS tracking to investigate
85 oceanographic drivers of habitat use in a piscivorous marine predator, the northern gannet *Morus*
86 *bassanus* (hereafter, 'gannet'). Gannets are large, medium-ranging marine predators, which feed on

87 a wide-variety of piscivorous prey (7, 39-41). Foraging plasticity in gannets has been linked to
88 oceanographic variability over a range of scales (40, 42-44). We here assess the influence of
89 mesoscale frontal activity on gannet foraging behaviour, and evaluate the utility of composite front
90 mapping for elucidating oceanographic controls of habitat selection. Moreover, we explicitly
91 address the importance of frontal persistence by investigating gannets' behavioural responses to
92 both contemporaneous and seasonally persistent thermal and chlorophyll fronts.

93

94 **2.0 METHODS**

95 **2.1 Device deployment**

96 Chick-rearing gannets (n=66) were tracked from a large breeding colony (~40,000 breeding pairs) on
97 Grassholm, Wales, UK (51° 43' N, 05° 28' W) over two breeding seasons (n=17, Jul 2010; n=49, Jun-
98 Jul 2011; Fig. 1). All birds were equipped with 30g GPS loggers (i-gotU; MobileAction Technology;
99 <http://www.i-gotu.com>), TESA-taped to feathers on the centre of the back. Previous studies indicate
100 these devices have no deleterious effects on foraging gannets (7). All birds were caught during
101 changeover at the nest, to minimise time chicks spent alone and to ensure foraging trips began
102 immediately following release. Handling time did not exceed 15 minutes. Devices were
103 programmed to record location fixes at one- or two- minute intervals, and recovered after at least
104 one complete foraging trip.

105 **FIGURE 1 HERE**

106

107 **2.2 Behavioural classification**

108 Area-Restricted Search (ARS) behaviour is characterised by low flight speed and frequent turning
109 (45) and can thus be distinguished from direct and fast transit to and from the colony. Previous
110 work has revealed that ARS is triggered by the detection and pursuit of prey in gannets (44). The
111 pelagic prey field is patchy and hierarchically organised, with dense prey patches nested within
112 broader-scale aggregation zones, and resultantly ARS is often observed at multiple nested scales (4,
113 6, 46, 47).

114

115 We used an approach based on residence time (RT; 48) to identify ARS bouts in all foraging tracks
116 (adehabitatLT R package; 49). To avoid artificial inflation of residence times, we excluded tracking
117 locations recorded during hours of darkness and all locations within a radius of 1km of the colony
118 (because gannets do not forage here but do frequently rest on the water). We then interpolated
119 each daylight movement bout to 60 second intervals and calculated RT at each of these locations,
120 using three radii (1km, 5km, 10km; 2 hours allowed outside circle before re-entering) to detect the

121 scale at which birds performed ARS. These radii were chosen to cover the range of ARS observed
122 previously in gannets (e.g. 44; average scale of search $9.1 \pm 1.9\text{km}$, with nested finer-scale search at
123 $1.5 \pm 0.8\text{km}$). We used RT at each interpolated location to distinguish ARS from transit using an
124 approach based on Lavielle segmentation (48) , using both the mean and variance of each series
125 with an 'Lmin' value of 3 (minimum number of observations in each segment) and a 'Kmax' value of
126 10 (maximum number of segments in movement burst; Supp. Fig. 1). We classified segments as
127 periods of ARS or transit using a custom-written R function that identifies each segment as either
128 above or below a threshold of residence time (seconds), with thresholds specified as mean values
129 across all trips at each radius, resulting in a binary response variable (i.e. ARS or transit) for each
130 radius (Supp. Fig. 2). We then used these multi-radii ARS classifications in subsequent analysis,
131 investigating levels of scale-dependence in the influence of fronts on habitat selection at meso- (10s
132 – 100s kms) and submeso- scales ($\sim 1\text{km}$).

133

134 **2.3 Composite front mapping**

135 Thermal composite front maps were created for the area enclosing accessible habitat (see 50; Fig. 2),
136 using a radius of whole-dataset maximum displacement from colony (432km). Firstly, raw (level 0)
137 Advanced Very High Resolution Radiometer (AVHRR) infrared data were converted to an index of
138 Sea-Surface Temperature (SST; level 2). SST data were then mapped on to the United Kingdom
139 Continental Shelf (UKCS) region in Mercator projection, with a spatial resolution of $\sim 1.1\text{km/pixel}$.
140 Thermal fronts were detected in each scene using Single-Image Edge Detection (SIED; 37).
141 Thresholds used for SIED front definition are often selected arbitrarily, and yet are central to
142 findings. We therefore actively varied the threshold for thermal front definition, enabling us to
143 objectively assess the effects on model predictions. To investigate the influence of the magnitude of
144 cross-frontal temperature gradient, we created separate thermal composite sets using 0.4°C and
145 1.0°C thresholds. All fronts detected over 7-day windows were included in composite front maps,
146 rolling by one day and covering the entire tracking duration. We also produced composite
147 chlorophyll-a (hereafter; chl-*a*) front maps from MODIS data using a similar protocol. However we
148 only used a single front detection threshold for chl-*a* owing to the log-space scale of chl-*a* imagery
149 ($0.06 \log \text{mg chl-a m}^{-3}$). Resultant composite maps (Fig. 2) quantify frontal activity using arbitrary
150 units (fcomp; 36), which are a combination of thermal gradient, persistence (ratio of front
151 observations to cloud-free views) and proximity of neighbouring fronts.

152

153 Composites were used to create a suite of metrics quantifying frontal activity designed for use with
154 tracking data (Fig. 2). We simplified the composite maps to determine contiguous contours through

155 the strongest front observations, using a novel clustering algorithm (Miller, *unpubl. data*) which first
156 involves smoothing the front map with a Gaussian filter of five pixels width. From these we
157 generated smoothed rasters describing distance to the closest front and frontal density, for use with
158 tracking data. **Frontal distance (fdist)** describes distance from any point to the closest simplified
159 front (Fig. 3). **Frontal density (fdens)** quantifies the relative strength of detected fronts, spatially
160 smoothed to give a continuous distribution of frontal activity (Fig. 3). We selected a smoothing
161 parameter based on the level of detail in resultant products, choosing a value that did not
162 oversmooth small-scale, ephemeral fronts. Thermal and chl-*a* front metrics were extracted for each
163 location along each track using custom software. In addition, we extracted surface chl-*a* (mg m^{-3} ; 7-
164 day composite) for each location, as an indicator of levels of primary production in relation to frontal
165 propagation.

166

167 Seasonal thermal front climatologies were also generated for each year (Jun-Aug; 2010-11), at
168 1.2km/pixel resolution. These **frequent front (ffreq)** maps (Fig. 4) identify seasonally persistent
169 frontal zones by highlighting regions in which strong, persistent or frequently-occurring fronts
170 manifest. We used a custom algorithm that estimates the percentage time in which a ‘strong’ front
171 (here, $F_{comp} \geq 0.015$) is detected within each grid cell over a specified time period (51). This F_{comp} unit
172 combines strength, persistence and proximity to other fronts (36), and this threshold is used to
173 exclude numerous weak and variable fronts that could confuse the seasonal frequency. Seasonal
174 chl-*a* (median) composites were created at the same temporal and spatial resolution, to highlight
175 areas of enhanced productivity in relation to persistent frontal zones.

176

177 **FIGURE 2 HERE**

178

179 **2.4 Modelling gannet foraging behaviour**

180 **2.4.1 Contemporaneous thermal and chlorophyll-*a* fronts**

181 First, we tested the influence of contemporaneous thermal and chl-*a* fronts on the probability of
182 observing ARS in gannets. Metrics describing frontal density (*fdens*), distance to closest simplified
183 front (*fdist*), and chl-*a* concentration were extracted from rolling 7-day composites centred at the
184 time of animal presence (Fig. 3). To account for the fact that gannet foraging range is influenced by
185 intra-specific interactions and travelling costs (52), we also included distance to the colony of each
186 GPS fix as a proportion of maximum displacement as a covariate in our models (50). All explanatory
187 covariates were standardised before inclusion by subtracting the mean and dividing by the standard
188 deviation (53). We checked for multi-collinearity using Generalised Variance Inflation Factors (GVIF)

189 and pairwise plots. Owing to observed colinearity, the *fdens* and *fdist* metrics were investigated
190 using separate models for both thermal and chl-*a* fronts.

191

192 To account for strong intra-individual temporal autocorrelation, we used Generalised Estimating
193 Equations (GEEs; 54), with each daylight movement bout as the blocking variable (see also 30, 55,
194 56). We constructed GEE-GAMs with a binomial error structure and logistic ('logit') link function
195 ('geepack' and 'splines' R packages;57). Quasi-likelihood under the model independence criterion
196 (QIC; 58) was used to select between a working independence correlation structure and an
197 autoregressive, AR1, correlation structure.

198

199 An approximated version of the QIC (QICu; 58) was used to select the most parsimonious set of
200 explanatory variables from *a priori* candidate models. In order to ascertain the most appropriate
201 form of each explanatory covariate, we compared the QICu of models with each term in its linear
202 form, and as a B-spline with 4 degrees of freedom and a knot positioned at the mean. QICu can be
203 over-conservative (59), so we used repeated Wald's tests to determine significance of retained
204 explanatory covariates.

205

206 Goodness-of-fit of final models was evaluated using a confusion matrix comparing binary predictions
207 to observed incidence of ARS in the original dataset. The probability cut-off above which a
208 prediction was classified as an ARS point was selected using a Receiver Operating Characteristic
209 (ROC) curve (60). We computed the area under the ROC curve (AUC) as a further measure of model
210 performance (closer to 1, better performance; 60). To obtain response curves, we predicted from
211 the final model for each of the explanatory terms, holding all other terms constant. Terms retained
212 by QICu model selection but found to be non-significant under more stringent Wald's tests were not
213 removed from the model (55), and only significant relationships were plotted.

214

215 **2.4.2 Seasonally persistent thermal and chlorophyll-*a* frontal zones**

216 Second, we tested the influence of seasonally persistent thermal and chl-*a* frontal zones (Fig. 4) on
217 gannet foraging habitat preference. As no intra-individual temporal autocorrelation existed in this
218 time-aggregated dataset, we used a binomial Generalised Additive Model (GAM) with a logistic
219 ('logit') link function to model presence/absence of ARS against front frequency for the 2011
220 breeding season ('mgcv' R package; 62). To achieve this, we created a grid at a matching spatial
221 resolution to the seasonal frequent front maps (1.2km; 'raster' R package;61), and then determined
222 presence/absence of ARS in each cell across all tracks. We were unable to do the same for 2010

223 because of low sample size. Environmental covariates were standardised before inclusion as
224 explanatory terms, and multi-collinearity was checked using GVIF and pairwise plots. Co-linearity
225 between the seasonal frequent front and chl-*a* metrics prevented simultaneous inclusion in the
226 same model, so the terms were applied separately. An index of habitat accessibility, derived using
227 the distance of each grid cell to the colony as a proportion of whole-dataset maximum displacement,
228 was also included to control for greater accessibility of fronts close to the colony than in fringes of
229 the foraging range (50).

230

231 In order to ascertain the best form for each explanatory covariate, we fitted separate models with
232 both linear and smoothed forms of each term, visualised the shape of smoothers and determined
233 the effect of the inclusion of each form on Akaike Information Criteria (AIC). Smoothers were only
234 included in final models where deemed biologically reasonable. For example, although the
235 smoothed forms of the front frequency metrics (mfreq; cfreq) were associated with lower AIC, linear
236 forms were preferred following visualisation of the smoother, as a conservative approach to prevent
237 over-fitting. Forwards and backwards step-wise model selection using AIC identified the final
238 model, which was then checked for overdispersion. Model residuals were checked for spatial
239 autocorrelation (53).

240

241 **3.0 RESULTS**

242 **3.1 Gannet foraging trips**

243 For the 66 birds tracked over the two breeding seasons, mean number of foraging trips was 3.8 ± 2.8
244 (range 1-12), with an average duration of 24.8 ± 22.7 hours (range 2 – 168 hours). The majority
245 (76%) involved one or more nights spent away from the colony (mode 1; range 0-7). Maximum
246 foraging range per trip ranged between 22.2 and 432.0 km from the colony, with an average of 178.3
247 ± 87.2 km. All foraging trips included at least one ARS zone.

248

249 **3.2 Contemporaneous thermal and chl-*a* fronts**

250 We found no evidence that gannet ARS was associated with contemporaneous thermal or
251 chlorophyll-*a* fronts, even when varying the threshold used for thermal front definition and the
252 radius used to define ARS through the residence time analysis. Although QICu model selection
253 retained contemporaneous front metrics in some model runs (Supp. Table 1), post-hoc repeated
254 Wald's tests confirmed that only distance to colony explained a significant proportion of deviance in
255 each of these model runs (Supp. Fig. 3).

256

257 Model validation confirmed goodness of fit of final models. True positive rates of model predictions,
258 obtained from confusion matrices, are given in Supplementary Table 1. ROC curves confirmed
259 models performed acceptably well. High levels of temporal autocorrelation (within-block
260 correlation, e.g. thermal 0.4°C threshold, 5km RT radius $fdens = 0.97 \pm 0.04$) justified the use of GEEs.
261 QIC comparison confirmed an AR1 autoregressive correlation structure as best fit for the data for all
262 models.

263

264

265 **FIGURE 3 HERE**

266

267 **TABLE 1 HERE**

268

269 **3.3 Seasonally persistent thermal and chl-a frontal zones**

270 Seasonal thermal front frequency (mfreq; Fig. 4a) was retained by model selection ($\chi^2_1 = 322.5$, $p <$
271 0.001 ; Fig. 4c; Table 2), with the probability of ARS twice as likely at high front frequency compared
272 with low (Fig. 4c). A smoothed relationship with habitat accessibility was also retained (HabAccess,
273 $df = 8$, $p < 0.001$; Supp. Fig. 4; Supp. Table 2). The model explained 33% of deviance and was not
274 over-dispersed (dispersion statistic = 0.83). Colinearity between thermal front frequency (Fig. 4a)
275 and seasonal average surface chl-*a* concentration also confirms that persistent frontal zones are
276 areas of increased primary productivity.

277

278 The seasonal front frequency index for chlorophyll-*a* fronts (cfreq; Fig. 4b) was also significant in
279 explaining the spatial distribution of ARS over the breeding season ($\chi^2_1 = 3108$, $p < 0.001$; Fig. 4d;
280 Supp. Table 2), alongside smoothed habitat accessibility ($p < 0.001$; Supp. Fig. 4; Supp. Table 2). The
281 model explained 32% of deviance and was not over-dispersed (dispersion statistic = 0.88).

282

283 **FIGURE 4 HERE**

284

285 **TABLE 2 HERE**

286

287 **4.0 DISCUSSION**

288 Combining composite front mapping with high-resolution GPS tracking, this work has revealed that
289 gannets are more likely to perform ARS within persistent mesoscale frontal zones than in other
290 regions of accessible habitat. This is of particular significance since it not only shows that mesoscale

291 fronts influence habitat selection, but also that remote sensing methods are able to identify features
292 relevant to piscivorous marine vertebrates. Moreover, this work also illustrates that temporal scale
293 is crucial - gannets do not tend to forage at ephemeral contemporaneous fronts, instead relying on
294 spatially predictable, seasonally persistent zones of frequent frontal activity.

295

296 **4.1. Mesoscale fronts and top predator foraging**

297 Predictability of foraging grounds is known to strongly influence seabird habitat selection, and may
298 partially explain our observed differences in front use (5). Many marine predators, including
299 seabirds, are known to repeatedly return to the same foraging areas (5, 7, 40, 63), which is generally
300 attributed to the presence of oceanographic features that are predictable in time and space. In the
301 Celtic Sea, these predictable foraging areas are associated with persistent mesoscale thermal and
302 chl-*a* frontal zones. The ultimate mechanisms by which these features are located are not known,
303 although a combination of memory effects, local enhancement and colonies acting as information
304 centres strongly influence observed foraging distributions in this species (52). Proximate
305 environmental factors enabling front detection include visual cues associated with the accumulation
306 of foam and detritus (18, 22); flow patterns, including surface convergence (22) and cross-frontal
307 jets (34), or olfactory cues such as dimethyl sulphide (DMS; 65). Persistent fronts probably produce
308 a stronger surface signal than ephemeral features, increasing detectability.

309

310 Alongside greater spatial predictability and detectability, persistent mesoscale frontal zones also
311 present more attractive foraging opportunities than ephemeral fronts. The bio-aggregative effects
312 of fronts vary with temporal persistence, spatial scale, temperature gradient, strength of convergent
313 flow and the properties of surrounding water masses, influencing their attractiveness as top
314 predator foraging habitat. Ephemeral, weak or spatially-variable features may not propagate for
315 sufficient time for biological enhancement to attract mid-trophic level consumers such as pelagic
316 fish. In contrast, persistent frontal zones are associated with sustained primary productivity, and
317 therefore more likely to attract the pelagic fish preyed upon by seabirds and other large marine
318 vertebrates.

319

320 In contrast to our findings, the closely-related Cape gannet *Morus capensis* is known to initiate ARS-
321 type behaviours at contemporaneous chl-*a* fronts in the Benguela (16). The reasons for these
322 differences are not clear, but are likely to be related to differences in regional oceanography. Small-
323 scale, superficial and ephemeral thermal fronts develop frequently in the Celtic Sea through tidal
324 effects and cycles of stratification and mixing (30), but are not always associated with chl-*a*

325 enrichment (28, 67). In contrast, the Benguela is a major upwelling zone, in which upwelling
326 filaments, eddies and strong vertically-structured fronts manifest. Although varying in seasonal
327 intensity and position, upwelling fronts in the Benguela are less spatiotemporally variable than tidal
328 fronts in the Celtic Sea over time scales of days to weeks, and so may be more predictable foraging
329 habitats for seabirds using learning and memory effects to locate prey (5). In addition, Cape
330 gannets prey upon the mega-abundant sardines and anchovies in the Benguela (16). These fish are
331 zooplanktivorous, and therefore more closely tied to oceanographic drivers, than the piscivorous fish
332 (e.g mackerel *Scomber scombrus*, garfish *Belone belone*) targeted by northern gannets in the Celtic
333 Sea (39). Differences in the biophysical nature of fronts encountered by prospecting birds within
334 these two contrasting oceanographic regions elicit different responses from these two closely-
335 related species. These differences highlight the need for a comprehensive understanding of regional
336 oceanography when investigating the drivers of habitat selection for mobile marine vertebrates.

337

338 Gannets in the Celtic Sea also forage extensively at fishing vessels (39,67, 68), so fisheries activity
339 could also influence the association between fronts and gannets reported here. Nevertheless, we
340 believe that gannets are using persistent frontal zones as natural foraging sites for the following
341 reasons. First, gannets switch between natural foraging and scavenging both within and among trips
342 (39) and must therefore rely upon both natural foraging and scavenging. Second, analysis of a
343 subset of ten gannets in 2011 equipped with bird-borne cameras enabled us to determine frontal
344 activity in the presence and absence of fishing vessels. This revealed little difference between
345 vessel-associated ARS instances, those associated with natural foraging and conditions experienced
346 during transit (see Supp. Fig. 5). Third, the majority of trawlers that gannets follow in the Celtic Sea
347 target demersal fish (39), which would not benefit from fishing in frontal regions.

348

349 **4.2. Composite front mapping and marine predator foraging habitat**

350 We have used multi-threshold objective front detection to produce composite thermal and chl-*a*
351 front maps at 1km resolution, enabling us to quantify the influence of fronts on foraging habitat
352 selection in gannets. Using this technique has negated sacrifice of tracking data as a result of cloud
353 cover. Furthermore, using both temporally-matched 7-day front composites and seasonal front
354 indices has revealed the importance of considering frontal persistence. However, composite front
355 mapping does have limitations with implications for defining marine predator foraging habitats. In
356 common with all remotely-sensed products, only the surface signature of complex three-
357 dimensional oceanographic processes is visible. Resolution of imagery is also limited by sensor
358 technology, restricting our ability to detect sub-mesoscale (~1km) nearshore tidal fronts, potentially

359 significant features in shallow shelf-seas (69). Furthermore, using 7-day composites could mask real-
360 time, fine-scale responses to environmental cues. Recent in-situ studies of fine-scale oceanographic
361 influence on seabird foraging have identified tidal state, thermal stratification index, and sub-surface
362 processes such as tidal shear at the thermocline, as significant influences on foraging decisions (55,
363 70). These fine-scale processes cannot be detected using contemporary remote sensing techniques.
364 However, remote sensing can provide oceanographic context for the movements of known
365 individuals over broader spatial and temporal scales, generating insights of direct relevance to
366 predictive habitat modelling (71) and marine spatial planning (51).

367

368 **5.0 CONCLUSIONS**

369 We here present proof of concept that objective front detection and composite front mapping (36)
370 can enhance the value of predator tracking data for habitat utilisation studies and improve
371 understanding of mechanistic links between oceanographic processes and marine vertebrate
372 foraging ecology. Novel front metrics used here provide capacity for quantification of the strength
373 of predator-frontal relationships without neglecting the significance of frontal strength, persistence
374 and scale. We have found that persistent frontal zones are preferred foraging habitats of a
375 piscivorous top predator inhabiting a shallow shelf sea, but that responses to contemporaneous
376 thermal and chl-*a* fronts vary. Persistent frontal zones are likely to represent predictably profitable
377 foraging grounds for predators that use learning and memory effects to locate prey. In contrast,
378 ephemeral, superficial fronts may not present attractive foraging opportunities owing to the spatial
379 and temporal lags inherent in bio-aggregation. Furthermore, persistent fronts are more likely to
380 generate environmental cues discernable to overflying gannets, and so more likely to become sites
381 of local enhancement for these network foragers. These findings provide direct evidence that the
382 temporal persistence of mesoscale fronts fundamentally regulates their value as foraging habitats
383 for marine predators.

384

385 Although considerable advances have been made in our understanding of the oceanographic drivers
386 of marine vertebrate habitat use in recent years, questions remain regarding the strength and
387 nature of predator-frontal associations. Our methods have considerable scope for further
388 application, providing opportunity for environmental contextualisation of habitat use, across
389 foraging guild, trophic level and oceanographic region. Composite front mapping allows us to
390 objectively detect thermal and chl-*a* fronts anywhere in the global ocean at high resolution, which
391 could help in locating critical at-sea habitats for mobile marine vertebrates, many of which are of
392 immediate conservation concern (72, 73). Furthermore, continuous near-real time global satellite

393 monitoring of environmental conditions, together with animal tracking and biologging, provides
394 capacity for investigation of responses to global change.

395 **ACKNOWLEDGEMENTS**

396 The authors thank Anthony Bicknell, James Grecian, Samantha Patrick, Greg and Lisa Morgan at
397 RSPB, and Tim Brooke at Venture Jet for logistical support. We thank Alain Zuur, David Pinaud and
398 David Sims for helpful discussions on technical aspects of analysis. This work was funded by the
399 Natural Environment Research Council (standard Grant NE/H007466/1) and the European Union (EU
400 Interreg CHARM III project) and carried out with appropriate permissions from the Royal Society for
401 the Protection of Birds (RSPB), the Countryside Commission for Wales (CCW) and the British Trust for
402 Ornithology (BTO).

403

404 **REFERENCES**

- 405 1. Weimerskirch H, Gault A, Cherel Y. Prey distribution and patchiness: factors in foraging success
406 and efficiency of wandering albatrosses. *Ecology*. 2005;86(10):2611-22.
- 407 2. Sims DW, Witt MJ, Richardson AJ, Southall EJ, Metcalfe JD. Encounter success of free-ranging
408 marine predator movements across a dynamic prey landscape. *Proceedings of the Royal Society
409 B: Biological Sciences*. 2006;273(1591):1195-201.
- 410 3. Fauchald P. Spatial interaction between seabirds and prey: review and synthesis. *Marine
411 Ecology Progress Series*. 2009;391:139-51.
- 412 4. Pinaud D, Weimerskirch H. At-sea distribution and scale-dependent foraging behaviour of
413 petrels and albatrosses: a comparative study. *Journal of Animal Ecology*. 2007;76(1):9-19.
- 414 5. Weimerskirch H. Are seabirds foraging for unpredictable resources? *Deep Sea Research Part II:
415 Topical Studies in Oceanography*. 2007;54(3-4):211-23.
- 416 6. Fauchald P, Tveraa T. Hierarchical patch dynamics and animal movement pattern. *Oecologia*.
417 2006;149(3):383-95.
- 418 7. Patrick SC, Bearhop S, Grémillet D, Lescroël A, Grecian WJ, Bodey TW, Hamer KC, Wakefield E,
419 Le Nuz M & Votier SC (2014) Individual differences in searching behaviour and spatial foraging
420 consistency in a central place marine predator. *Oikos* 123: 33-40
- 421 8. Broderick AC, Coyne MS, Fuller WJ, Glen F, Godley BJ. Fidelity and over-wintering of sea turtles.
422 *Proceedings of the Royal Society B: Biological Sciences*. 2007;274(1617):1533.
- 423 9. Bradshaw CJA, Hindell MA, Sumner MD, Michael KJ. Loyalty pays: potential life history
424 consequences of fidelity to marine foraging regions by southern elephant seals. *Animal
425 Behaviour*. 2004;68(6):1349-60.

- 426 10. Hays GC, Hobson VJ, Metcalfe JD, Righton D, Sims D. Flexible foraging movements of
427 leatherback turtles across the North Atlantic Ocean. *Ecology*. 2006;87(10):2647-56.
- 428 11. Bost CA, Cotté C, Bailleul F, Cherel Y, Charrassin JB, Guinet C, et al. The importance of
429 oceanographic fronts to marine birds and mammals of the southern oceans. *Journal of Marine*
430 *Systems*. 2009;78(3):363-76.
- 431 12. Polovina JJ, Howell E, Kobayashi D, Seki MP. The transition zone chlorophyll front, a dynamic
432 global feature defining migration and forage habitat for marine resources. *Progress in*
433 *Oceanography*. 2001;49(469-483).
- 434 13. Doniol-Valcroze T, Berteaux D, Larouche P, Sears R. Influence of thermal fronts on habitat
435 selection by four rorqual whale species in the Gulf of St. Lawrence. *Marine Ecology Progress*
436 *Series*. 2007;335:207-16.
- 437 14. Sims D, Southall EJ, Richardson AJ, Reid PC, Metcalfe JD. Seasonal movements and behaviour of
438 basking sharks from archival tagging: no evidence of winter hibernation. *Marine Ecology*
439 *Progress Series*. 2003;248(187-196).
- 440 15. Godø OR, Samuelson A, Macaulay GJ, Patel R, Hjøllø SS, Horne J, et al. Mesoscale eddies are
441 oases for higher trophic marine life. *PLoS ONE*. 2012;7(1):e30161.
- 442 16. Sabarros PS, Grémillet D, Demarcq H, Moseley C, Pichegru L, Mullers RH, et al. Fine-scale
443 recognition and use of mesoscale fronts by foraging Cape gannets in the Benguela upwelling
444 region. *Deep Sea Research Part II: Topical Studies in Oceanography*. 2013.
- 445 17. Tew Kai E, Rossi V, Sudre J, Weimerskirch H, Lopez C, Hernandez-Garcia E, et al. Top marine
446 predators track Lagrangian coherent structures. *Proceedings of the National Academy of*
447 *Sciences*. 2009;106(20):8245.
- 448 18. Le Fevre J. Aspects of the biology of frontal systems. *Advances in Marine Biology*. 1986;23:164-
449 299.
- 450 19. Belkin IM, Cornillon PC, Sherman K. Fronts in large marine ecosystems. *Progress in*
451 *Oceanography*. 2009;81(1):223-36.
- 452 20. Franks PJS. Phytoplankton blooms at fronts: patterns, scales, and physical forcing mechanisms.
453 *Reviews in Aquatic Sciences*. 1992;6(2):121-37.
- 454 21. Genin A, Jaffe JS, Reef R, Richter C, Franks PJS. Swimming Against the Flow: A Mechanism of
455 Zooplankton Aggregation. *Science*. 2005;308:860-2.
- 456 22. Franks PJS. Sink or swim: accumulation of biomass at fronts. *Marine Ecology Progress Series*.
457 1992;82:1-12.
- 458 23. Yoder JA, Ackleson SG, Barber RT, Flament P, Balch WM. A line in the sea. *Nature*.
459 1994;371:689-92.

- 460 24. Owen RW. Fronts and Eddies in the Sea: Mechanisms, Interactions and Biological Effects. In:
461 Longhurst AR, editor. Analysis of marine ecosystems. New York: Academic Press; 1981. p. 197-
462 233.
- 463 25. Gregory Lough R, Manning JP. Tidal-front entrainment and retention of fish larvae on the
464 southern flank of Georges Bank. Deep Sea Research Part II: Topical Studies in Oceanography.
465 2001;48(1-3):631-44.
- 466 26. Sabatés A, Masó M. Effect of a shelf-slope front on the spatial distribution of mesopelagic fish
467 larvae in the western Mediterranean. Deep Sea Research Part A Oceanographic Research
468 Papers. 1990;37(7):1085-98.
- 469 27. Godley B, Bearhop S, Cooke S, Dixson A, Hodgson D, Marsh H, et al. Tracking vertebrates for
470 conservation. Endangered Species Research [Special Issue]. 2008;4(1-2).
- 471 28. Scott BE, Sharples J, Ross ON, Wang J, Pierce GJ, Camphuysen CJ. Sub-surface hotspots in
472 shallow seas: fine-scale limited locations of top predator foraging habitat indicated by tidal
473 mixing and sub-surface chlorophyll. Marine Ecology Progress Series. 2010;408:207-26.
- 474 29. Embling CB, Illian J, Armstrong E, van der Kooij J, Sharples J, Camphuysen KCJ, et al.
475 Investigating fine-scale spatio-temporal predator–prey patterns in dynamic marine ecosystems:
476 a functional data analysis approach. Journal of Applied Ecology. 2012; 49: 481-492.
- 477 30. Pirotta E, Thompson PM, Miller PI, Brookes KL, Cheney B, Barton TR, et al. Scale-dependent
478 foraging ecology of a marine top predator modelled using passive acoustic data. Functional
479 Ecology. 2014; 28(1):206-217.
- 480 31. Hunt Jr GL, Russell RW, Coyle KO, Weingartner T. Comparative foraging ecology of planktivorous
481 auklets in relation to ocean physics and prey availability. Marine Ecology Progress Series.
482 1998;167:241-59.
- 483 32. Block BA, Jonsen ID, Jorgensen SJ, Winship AJ, Shaffer SA, Bograd SJ, et al. Tracking apex marine
484 predator movements in a dynamic ocean. Nature. 2011;475(7354):86-90.
- 485 33. Grémillet D, Lewis S, Drapeau L, van Der Lingen CD, Huggett JA, Coetzee JC, et al. Spatial match–
486 mismatch in the Benguela upwelling zone: should we expect chlorophyll and sea-surface
487 temperature to predict marine predator distributions? Journal of Applied Ecology. 2008;45:610-
488 21.
- 489 34. Simpson JH, Sharples J. Introduction to the physical and biological oceanography of shelf seas.
490 Cambridge: Cambridge University Press; 2012.
- 491 35. Durazo R, Harrison N, Hill A. Seabird observations at a tidal mixing front in the Irish Sea.
492 Estuarine, Coastal and Shelf Science. 1998;47(2):153-64.

- 493 36. Miller P. Composite front maps for improved visibility of dynamic sea-surface features on
494 cloudy SeaWiFS and AVHRR data. *Journal of Marine Systems*. 2009;78(3):327-36.
- 495 37. Cayula J-F, Cornillon PC. Edge detection algorithm for SST images. *Journal of Atmospheric and*
496 *Oceanic Technology*. 1992;9:67-80.
- 497 38. Graham RT, Witt MJ, Castellanos DW, Remolina F, Maxwell S, Godley BJ, et al. Satellite tracking
498 of manta rays highlights challenges to their conservation. *PLoS ONE*. 2012;7(5):e36834.
- 499 39. Votier SC, Bicknell A, Cox SL, Scales KL, Patrick SC. A bird's eye view of discard reforms: bird-
500 borne cameras reveal seabird/fishery interactions. *PLoS ONE*. 2013;8(3):e57376.
- 501 40. Hamer K, Humphreys E, Garthe S, Hennicke J, Peters G, Grémillet D, et al. Annual variation in
502 diets, feeding locations and foraging behaviour of gannets in the North Sea: flexibility,
503 consistency and constraint. *Marine Ecology Progress Series*. 2007;338(2):5-305.
- 504 41. Martin A. The diet of Atlantic Puffin *Fratercula arctica* and Northern Gannet *Sula bassana* chicks
505 at a Shetland colony during a period of changing prey availability. *Bird Study*. 1989;36(3):170-
506 80.
- 507 42. Garthe S, Montevecchi WA, Chapdelaine G, Rail JF, Hedd A. Contrasting foraging tactics by
508 northern gannets (*Sula bassana*) breeding in different oceanographic domains with different
509 prey fields. *Marine Biology*. 2007;151(2):687-94.
- 510 43. Garthe S, Montevecchi WA, Davoren GK. Inter-annual changes in prey fields trigger different
511 foraging tactics in a large marine predator. *Limnology and Oceanography*. 2011;56:802-12.
- 512 44. Hamer K, Humphreys E, Magalhaes M, Garthe S, Hennicke J, Peters G, et al. Fine-scale foraging
513 behaviour of a medium-ranging marine predator. *Journal of Animal Ecology*. 2009;78(4):880-9.
- 514 45. Pinaud D. Quantifying search effort of moving animals at several spatial scales using first-
515 passage time analysis: effect of the structure of environment and tracking systems. *Journal of*
516 *Applied Ecology*. 2008;45(1):91-9.
- 517 46. Fauchald P, Erikstad KE, Skarsfjord H. Scale-dependent predator-prey interactions: the
518 hierarchical spatial distribution of seabirds and prey. *Ecology*. 2000;81(3):773-83.
- 519 47. Fauchald P, Tveraa T. Using first-passage time in the analysis of area-restricted search and
520 habitat selection. *Ecology*. 2003;84(2):282-8.
- 521 48. Barraquand F, Benhamou S. Animal movements in heterogenous landscapes: identifying
522 profitable places and homogenous movement bouts. *Ecology*. 2008;89(12):3336-48.
- 523 49. Calenge C. The package adehabitat for the R software: a tool for the analysis of space and
524 habitat use by animals. *Ecological Modelling*. 2006;197:516-9.

- 525 50. Wakefield ED, Phillips RA, Matthiopoulos J. Quantifying habitat use and preferences of pelagic
526 seabirds using individual movement data: a review. *Marine Ecology Progress Series*.
527 2009;391:165-82.
- 528 51. Miller PI, Christodoulou S. Frequent locations of ocean fronts as an indicator of pelagic diversity:
529 application to marine protected areas and renewables. *Marine Policy*. 2013.
- 530 52. Wakefield ED, Bodey TW, Bearhop S, Blackburn J, Colhoun K, Davies R, Dwyer RG, Green J,
531 Grémillet D, Jackson AL (2013) Space Partitioning Without Territoriality in Gannets. *Science*
532 341(6141):68-70.
- 533 53. Zuur A. *A Beginner's Guide to Generalized Additive Models with R*. Newburgh: Highland
534 Statistics Ltd.; 2012.
- 535 54. Liang K-Y, Zeger SL. Longitudinal data analysis using generalized linear models. *Biometrika*.
536 1986;73(1):13-22.
- 537 55. Pirotta E, Matthiopoulos J, MacKenzie M, Scott-Hayward L, Rendell L. Modelling sperm whale
538 habitat preference: a novel approach combining transect and follow data. *Marine Ecology*
539 *Progress Series*. 2011;436:257-72.
- 540 56. Scott B, Webb A, Palmer M, Embling C, Sharples J. Fine scale bio-physical oceanographic
541 characteristics predict the foraging occurrence of contrasting seabird species; Gannet (*Morus*
542 *bassanus*) & Storm Petrel (*Hydrobates pelagicus*). *Progress in Oceanography*. 2013.
- 543 57. Højsgaard S, Halekoh U, Yan J. The R package geepack for Generalized Estimating Equations.
544 *Journal of Statistical Software*. 2006;15(2):1-11.
- 545 58. Pan W. Akaike's information criterion in generalized estimating equations. *Biometrics*.
546 2004;57(1):120-5.
- 547 59. Hardin JW, Hilbe JM. *Generalized Estimating Equations (GEE)*. Boca Raton, Florida: Chapman &
548 Hall/CRC; 2003.
- 549 60. Zweig MH, Campbell G. Receiver-operating characteristic (ROC) plots: a fundamental evaluation
550 tool in clinical medicine. *Clinical chemistry*. 1993;39(4):561-77.
- 551 61. Hijmans RJ, van Etten J. raster: Geographic analysis and modelling with raster data. R package
552 version 2.0-8 <http://CRAN.R-project.org/package=raster>. 2012.
- 553 62. Wood SN. *Generalized Additive Models: An Introduction with R*.: Chapman and Hall/CRC; 2006.
- 554 63. Pettex E, Bonadonna F, Enstipp M, Siorat F, Grémillet D. Northern gannets anticipate the
555 spatio-temporal occurrence of their prey. *Journal of Experimental Biology*. 2010;213(14):2365-
556 71.

- 557 64. Tremblay Y, Thiebault A, Mullers R, Pistorius P (2014) Bird-Borne Video-Cameras Show That
558 Seabird Movement Patterns Relate to Previously Unrevealed Proximate Environment, Not Prey.
559 PLoS ONE 9:e88424
- 560 65. Nevitt GA, Bonadonna F. Sensitivity to dimethyl sulphide suggests a mechanism for olfactory
561 navigation by seabirds. *Biology letters*. 2005;1(3):303-5.
- 562 66. Pemberton K, Rees AP, Miller PI, Raine R, Joint I. The influence of water body characteristics on
563 phytoplankton diversity and production in the Celtic Sea. *Continental shelf research*.
564 2004;24(17):2011-28.
- 565 67. Votier, S.C., Bearhop, S., Witt, M.J., Inger, R., Thompson, D. & Newton, J. Individual responses of
566 seabirds to commercial fisheries revealed using GPS tracking, stable isotopes and vessel
567 monitoring systems. *Journal of Applied Ecology*. 2010;47:487-497.
- 568 68. Bodey, T.W., Jessopp, M.J., Votier, S.C., Gerritsen, H.D., Cleasby, I.R., Hamer, K.C., Patrick, S.C.,
569 Wakefield, E.D. & Bearhop, S. Seabird movement reveals the ecological footprint of fishing
570 vessels. *Current Biology*. 2014; 24:514-515.
- 571 69. Mendes S, Turrell W, Lütkebohle T, Thompson PM. Influence of the tidal cycle and a tidal
572 intrusion front on the spatio-temporal distribution of coastal bottlenose dolphins. *Marine
573 Ecology Progress Series*. 2002;239:221-9.
- 574 70. Cox S, Scott B, Camphuysen C. Combined spatial and tidal processes identify links between
575 pelagic prey species and seabirds. *Marine Ecology Progress Series*. 2013;479:203-21.
- 576 71. Oppel S, Meirinho A, Ramírez I, Gardner B, O'Connell AF, Miller PI, et al. Comparison of five
577 modelling techniques to predict the spatial distribution and abundance of seabirds. *Biological
578 Conservation*. 2012;156(0):94-104.
- 579 72. Croxall JP, Butchart SHM, Lascelles B, Stattersfield AJ, Sullivan B, Symes A, et al. Seabird
580 conservation status, threats and priority actions: a global assessment. *Bird Conservation
581 International*. 2012;22(01):1-34.
- 582 73. Myers RA, Worm B. Rapid worldwide depletion of predatory fish communities. *Nature*.
583 2003;423(6937):280-3.
- 584

585 **FIGURE AND TABLE CAPTIONS**

586 **FIGURES**

587 **Fig. 1. GPS tracking.** All foraging trips of birds GPS-tracked during 2010 (a, n=17) and 2011 breeding
588 seasons (b, n=49). Grassholm colony shown as grey star.
589

590

591 **Fig. 2. Composite front mapping.** Preparation of thermal composite front maps, and front metrics
592 rasters, from Advanced Very High Resolution Radiometer (AVHRR) sea surface temperature (SST)
593 images. Several satellite passes per day are mapped to the study area (e.g. a,b). Single-Image Edge
594 Detection (SIED) detects fronts in each of these swaths, using a given threshold for front definition,
595 here 0.4°C (c,d). Composite front maps are created from all fronts detected in imagery over a 7-day
596 period (e; Miller, 2009), and spatially smoothed to generate a frontal density (*fdens*) metric (f) or
597 simplified to generate a distance to closest front (*fdist*) metric (g).

598

599 **Fig. 3. Contemporaneous front metrics time-matched to gannet foraging trip.** Distance to closest
600 thermal front (*fdist*; 0.4°C threshold, a), thermal front density (*fdens*; 0.4°C threshold, b), distance to
601 closest chl-*a* front (c) and chl-*a* front density (d) shown for one complete foraging trip (23 July 2011).
602 Points designated as ARS by residence time analysis (5km radius) shown as white track sections, and
603 transit as black track sections. Colony location shown as black star.

604

605 **Fig. 4. Modelling the effects of persistent frontal zones (thermal, chl-*a*) on the spatial distribution**
606 **of gannet area-restricted search behaviour.** Seasonally persistent (Jun-Aug 2011) thermal frontal
607 zones (a) and chl-*a* frontal zones (b), identified using frequent front (*mfreq*; *cfreq*) metrics. Model
608 predictions for effects of seasonal thermal front frequency (c; model 4.1) and seasonal chl-*a* front
609 frequency (d; model 4.2). Gannets are more likely to perform ARS behaviours within regions of
610 frequent frontal activity.

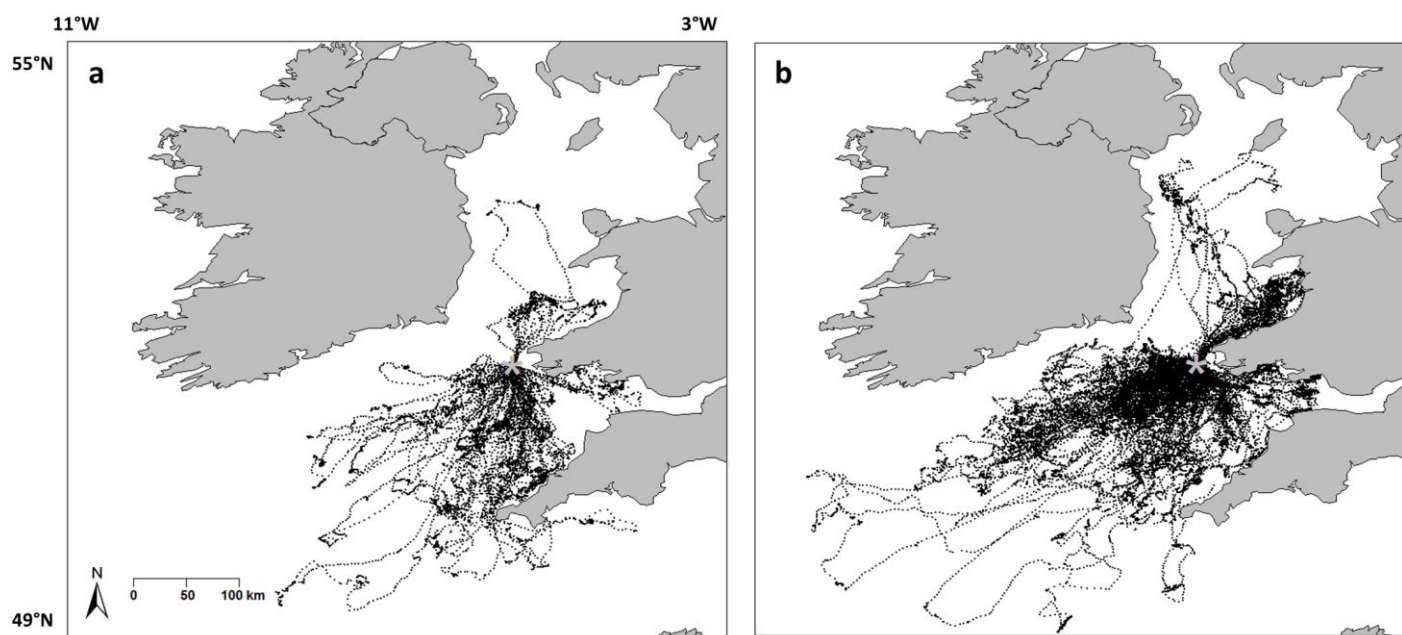


Fig. 1. GPS tracking. All foraging trips of birds GPS-tracked during 2010 (a, n=17) and 2011 breeding seasons (b, n=49). Grassholm colony shown as grey star.

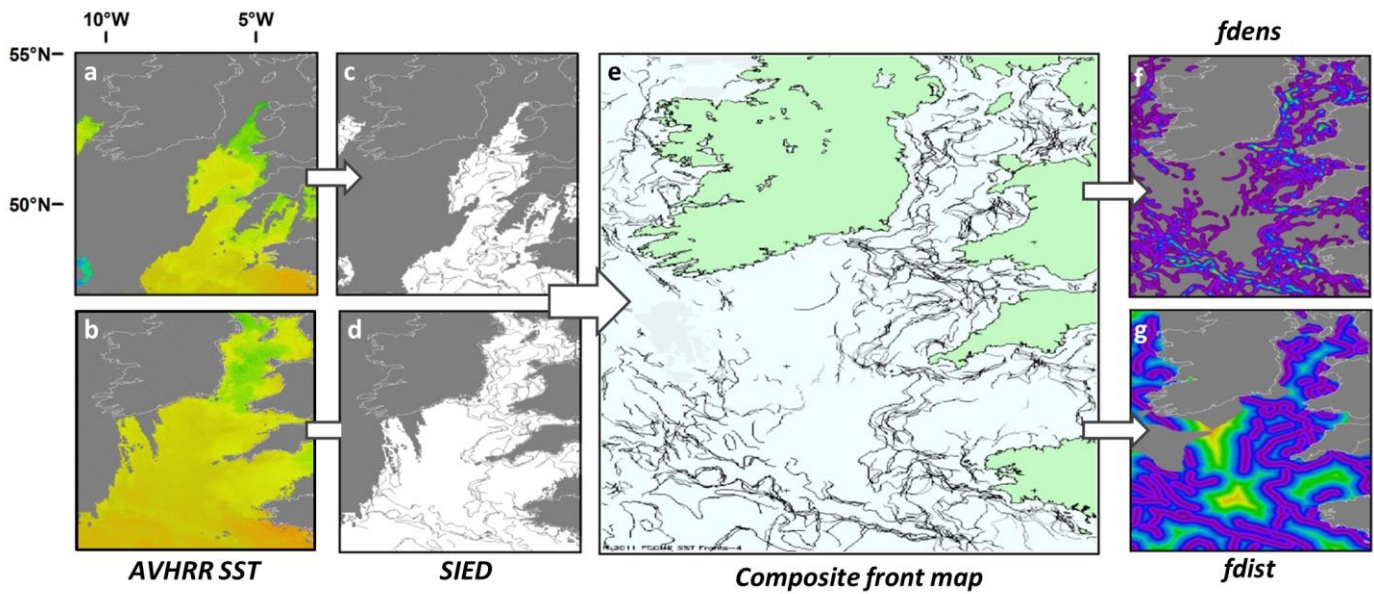


Fig. 2. Composite front mapping. Preparation of thermal composite front maps, and front metrics rasters, from Advanced Very High Resolution Radiometer (AVHRR) sea surface temperature (SST) images. Several satellite passes per day are mapped to the study area (e.g. a,b). Single-Image Edge Detection (SIED) detects fronts in each of these swaths, using a given threshold for front definition, here 0.4°C (c,d). Composite front maps are created from all fronts detected in imagery over a 7-day period (e; Miller, 2009), and spatially smoothed to generate a frontal density (*fdens*) metric (f) or simplified to generate a distance to closest front (*fdist*) metric (g).

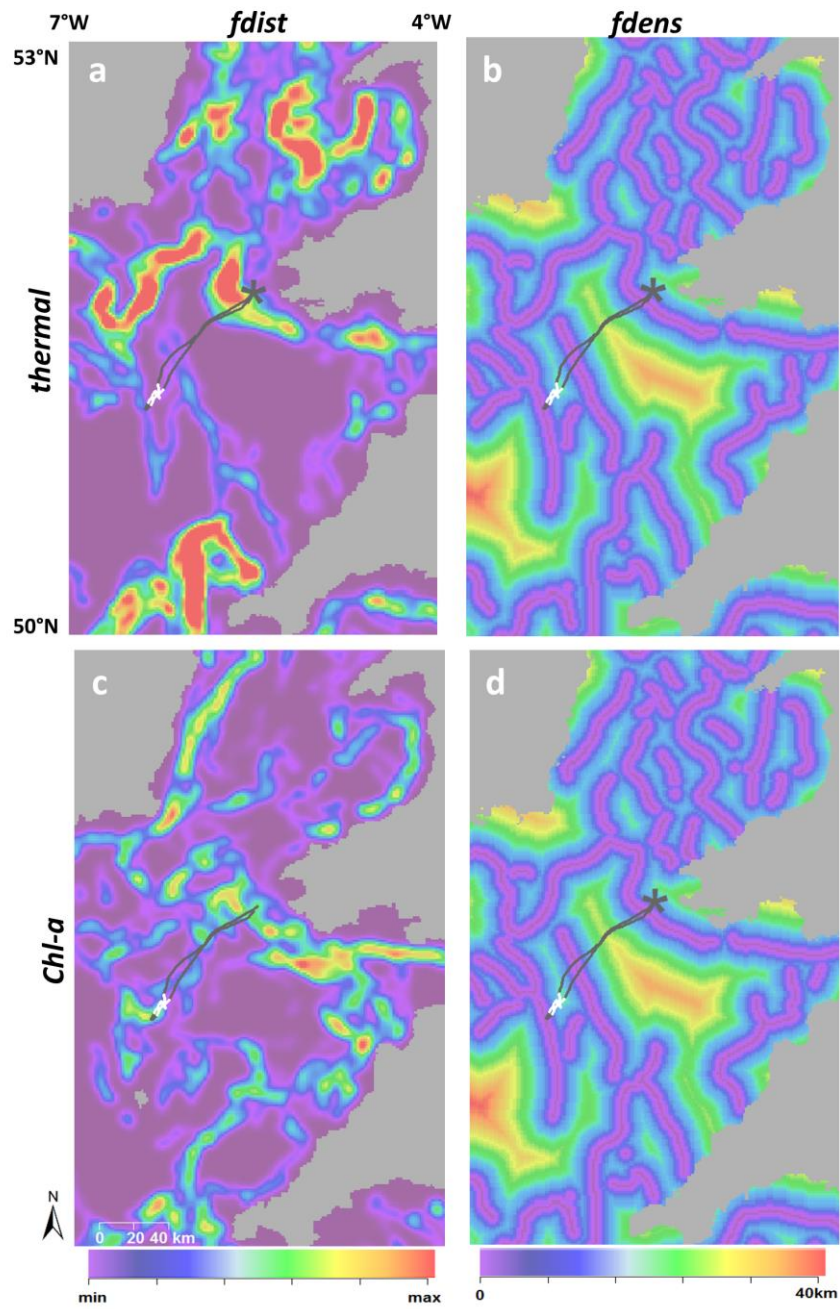


Fig. 3. Contemporaneous front metrics time-matched to gannet foraging trip. Thermal front density (*fdens*; 0.4°C threshold, a), distance to closest thermal front (*fdist*; 0.4°C threshold, b), chl-*a* front density (d) and distance to closest chl-*a* front (d) shown for one complete foraging trip (23 July 2011). Points designated as ARS by residence time analysis (5km radius) shown as white track sections, and commuting flight as black track sections. Colony location shown as black star.

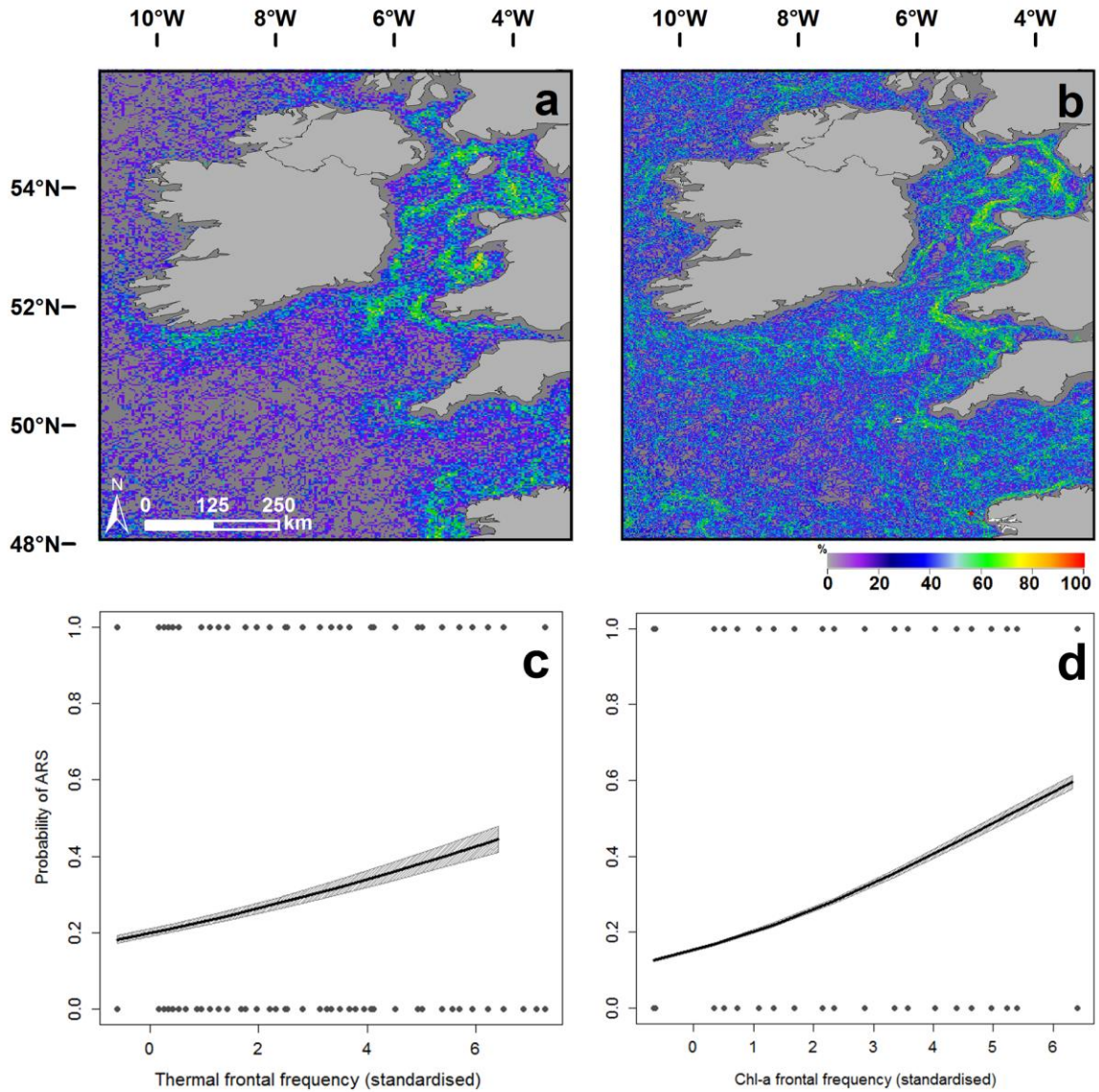
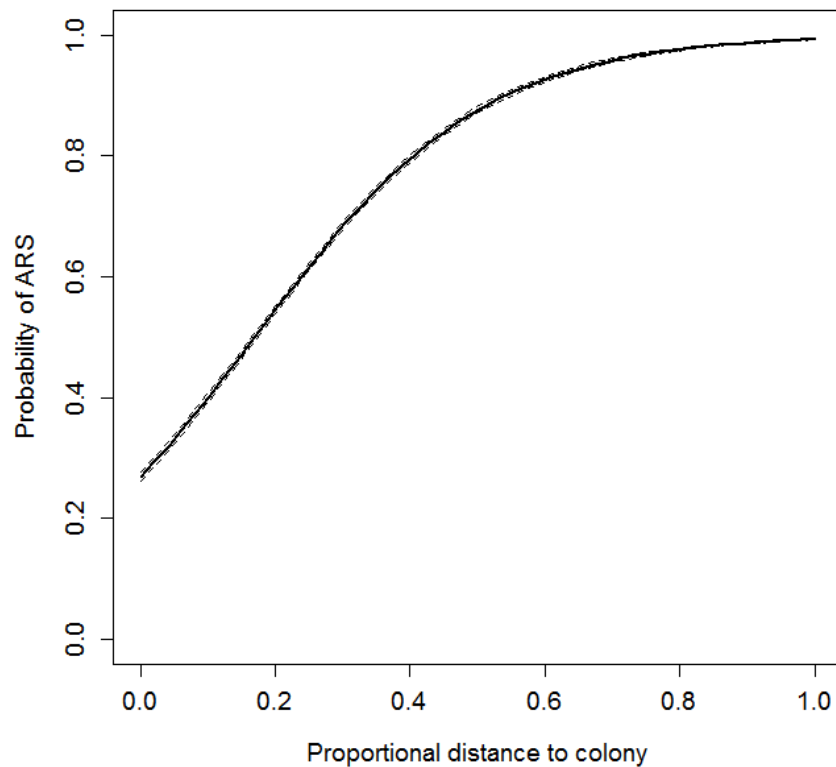
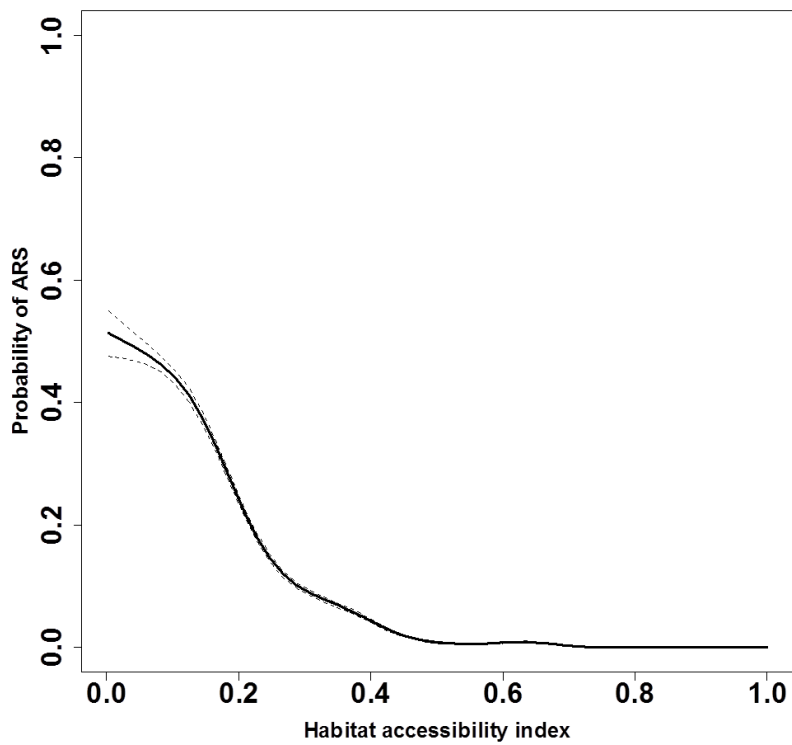


Fig. 4. Modelling the effects of persistent frontal zones (thermal, chl-a) on the spatial distribution of gannet area-restricted search behaviour. Seasonally persistent (Jun-Aug 2011) thermal frontal zones (a) and chl-a frontal zones (b), identified using frequent front (mfreq; cfreq) metrics. Model predictions for effects of seasonal thermal frontal frequency (c; model 4.1) and seasonal chl-a frontal frequency (d; model 4.2). Gannets are more likely to perform ARS behaviours within regions of frequent frontal activity.



Supplementary Fig. 1. Modelling the effects of contemporaneous thermal fronts on gannet area-restricted search behaviour, using GEE-GAMs. Contemporaneous front GEE-GAM results (model 1.1.2), showing predicted influence of proportional distance to colony. All other explanatory terms, including thermal and chlorophyll front metrics, were not statistically significant, so are not shown here. The higher probability of ARS further from the colony represents the tendency for ARS zones to take place at the distal point of foraging points, as ARS 0/1 along each track was used as the response variable. Confidence Intervals represented by dashed lines, here close to the main effect line, owing to small standard error on this coefficient estimate in model output.



Supplementary Fig. 2. Modelling the effects of persistent frontal zones (thermal, chl-a) on the spatial distribution of gannet area-restricted search behaviour. Habitat Accessibility index fitted to binomial GAM investigating the influence of persistent frontal zones on gannet ARS behaviour (models 4.1, 4.2) as a control for availability of fronts as a function of distance from colony.